Available online at www.sciencedirect.com
ScienceDirect
Tetrahedron
Tetrahedron 63 (2007) 9970–9978

Aplysiols A and B, squalene-derived polyethers from the mantle of the sea hare *Aplysia dactylomela*

Emiliano Manzo,[a,*] Margherita Gavagnin,[a] Giuseppe Bifulco,[b] Paola Cimino,[b] Simone Di Micco,[b] M. Letizia Ciavatta,[a] Yue Wei Guo[c] and Guido Cimino[a]

[a]*Istituto di Chimica Biomolecolare, CNR, Via Campi Flegrei 34, 80078 Pozzuoli, Naples, Italy*
[b]*Dipartimento di Scienze Farmaceutiche, Universita' di Salerno, Via Ponte Don Melillo, 84084 Fisciano, Salerno, Italy*
[c]*State Key Laboratory of Drug Research, Institute of Materia Medica, Shanghai Institutes for Biological Sciences, Chinese Academy of Sciences, 201203 Shanghai, China*

Received 2 May 2007; revised 5 July 2007; accepted 19 July 2007
Available online 26 July 2007

Abstract—Two novel triterpenoids, aplysiols A (**5**) and B (**6**), have been isolated, together with structurally related known metabolites, from a South China Sea collection of the anaspidean mollusc *Aplysia dactylomela*. The structures of **5** and **6** were determined mainly by spectroscopic NMR techniques. The absolute stereochemistry of compound **5** was deduced by Mosher's method as well as by biogenetical consideration, whereas the absolute stereochemistry of compound **6** was established also using an integrated NMR-QM (Quantum Mechanical) approach, based on the combination of ^{13}C NMR chemical shifts and $^{2,3}J_{C-H}$ coupling constant DFT (density functional theory) calculations.

1. Introduction

Squalene-derived polyethers exhibiting a dioxabicyclo[4,4,0]decane ring represent a very interesting group of metabolites of *Laurencia* red algae.[1,2] The first example of this biogenetically unique class was thyrsiferol (**1**), isolated from *Laurencia thyrsifera* by Blunt et al. in 1978.[3] Subsequently, a series of related triterpenoids differing at C-15/C-24 moiety either in the stereochemistry of chiral centres (i.e., venustatriol, **2**[4]) or in the oxidation degree (i.e., 16-hydroxydehydrothyrsiferol, **3**[5]) or in the structural arrangement (i.e., isodehydrothyrsiferol, **4**[6]) have been reported from several *Laurencia* species. A limited number of related molecules with structural differences in the ring A have also been isolated.[5] The original structural features[1] as well as the potent antiviral,[4] cytotoxic[7] and inhibitory[8] effects possessed by these molecules generated many synthetic efforts directed towards their producing.[9] Surprisingly, these triterpenes were never found in opisthobranch molluscs, even though some species, belonging to the *Aplysia* genus, usually eat upon red algae.[10]

In the course of our research on bioactive secondary metabolites of marine organisms, we recently analysed specimens of the sea hare *Aplysia dactylomela* collected from South China Sea.[11] This study led to the isolation of unprecedented C_{15}-halogenated acetogenins, structurally related to typical metabolites of red algae of the genus *Laurencia*. On this basis, and according to the chemical data reported in the literature[2,11] for *A. dactylomela*, a probable dietary origin of these molecules from a *Laurencia* species was suggested. In addition, mixtures of polar terpenoids were also detected in the ether extracts of both the skin and the internal organs of the mollusc, but not further investigated.[11]

We report here the chemical analysis of these more polar fractions that has resulted in the isolation of two new triterpene polyethers, aplysiol A (**5**) and aplysiol B (**6**), structurally related to the co-occurring thyrsiferol (**1**) and venustatriol (**2**). The structures of **5** and **6** have been determined by extensive 2D-NMR studies. The configuration of the stereogenic centres of the C-15/C-24 portion of aplysiol B (**6**) has been deduced by an integrated NMR-QM (Quantum Mechanical) approach, while the absolute stereochemistry of compounds **5** and **6** has been assigned as reported by biogenetical correlation with **1**, the absolute configuration of which was secured by stereospecific synthesis (Hashimoto et al.), as well as by Mosher's method.

2. Results and discussion

A polar terpenoid fraction (R_f 0.20–0.40, $CHCl_3$/MeOH 95:5) was obtained from ether extracts of both mantle and internal organs,[11] even though the amount of this fraction was significantly different in the two parts (34 mg from

Keywords: Marine natural products; Molluscs; Aplysiol; Absolute stereochemistry.
* Corresponding author. Tel.: +39 081 8675177; fax: +39 081 8041770; e-mail: emanzo@icmib.na.cnr.it

0040–4020/$ - see front matter © 2007 Published by Elsevier Ltd.
doi:10.1016/j.tet.2007.07.055

the mantle, 5% of the extract; 16 mg from the internal organs, 0.1% of the extract). Preliminary ^{1}H NMR spectroscopic analysis of the two fractions revealed that they were mixtures of oxygenated triterpenes with a different composition, in particular the mixture deriving from the mantle extract (F_m) was more complex with respect to that obtained from the extract of the internal organs (F_i). Therefore, the two fractions were separately purified by silica gel column chromatography (petroleum ether/diethyl ether gradient and subsequently $CHCl_3$/MeOH, 95/5). Pure venustatriol (**2**) and thyrsiferol (**1**) were obtained, in order of polarity, from both fractions (0.3 and 1.1 mg, respectively, from F_i, and 0.7 and 4.9 mg, respectively, from F_m), whereas an additional main mixture of related compounds (21 mg) was obtained from F_m. This mixture was further purified by reverse phase HPLC (MeOH/H_2O, 85/15) giving, in order of retention time, two new compounds, named aplysiol A (**5**, 7.0 mg) and aplysiol B (**6**, 9.0 mg).

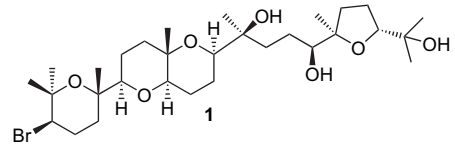

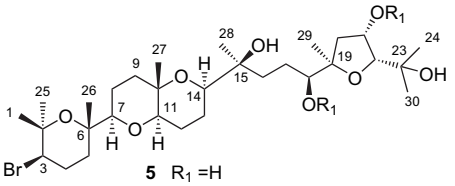

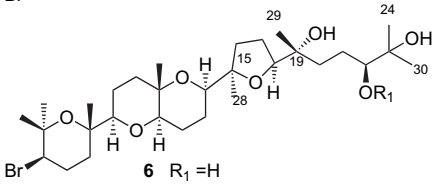

(+)-Thyrsiferol (**1**) and (+)-venustatriol (**2**) were identified by comparison of their spectral data (NMR, MS, $[\alpha]_D$) with the literature.[3,4,12] A detailed 2D-NMR spectroscopic analysis was conducted on thyrsiferol (**1**) (see Table 1) leading to a re-assignment of the NMR values for some methyl and methylene groups, incorrectly attributed in Ref. 12. In particular, proton and carbon values of C-16, C-26 and C-28 should be inverted with those of C-20, C-27 and C-29, respectively, as it was indicated by a series of diagnostic correlations in the HMBC spectrum of **1**.

Aplysiols A (**5**) and B (**6**) were the main triterpenes selectively located on the mantle of the mollusc. Preliminary ^{1}H NMR spectroscopic analysis of these metabolites revealed a close relationship with the co-occurring **1** and **2**, in particular displaying the presence of the partial structure with bromine-containing pyran linked to a dioxabicyclo[4,4,0]decane ring on the left side of the molecule (Table 1).

The molecular formula of **5**, $C_{30}H_{53}BrO_8$, deduced by HRESIMS on the sodiated molecular ion peak at 643.2828, contained an additional oxygen atom with respect to compounds **1** and **2**.

Comparison of ^{1}H and ^{13}C NMR spectra of aplysiol A (**5**) with those of thyrsiferol (**1**)[3] confirmed the presence of the same carbon skeleton displaying in **5** an additional secondary hydroxyl substituent at the terminal tetrahydrofuran ring. In fact, careful analysis of their ^{1}H–^{1}H COSY and HSQC spectra revealed the presence of spin systems between C-15 and C-19 almost identical to those of thyrsiferol (**1**) (Table 1). The terminal moiety of the molecule exhibited a carbinol proton at δ 4.45 (br s, H-21), which was correlated to both a methylene at δ 1.81 (m, H-20a) and δ 2.20 (m, H-20b), and a methine at δ 3.57 (d, J=1.5 Hz, H-22), which were not further coupled, supporting the location of the secondary hydroxyl group on the tetrahydrofuran ring as reported in formula **5**. Accordingly, diagnostic HMBC correlations were observed between C-19 (δ 86.0) and H-18, H_2-20 and H_3-29, and between C-22 (δ 87.0) and H-21, H_3-24 and H_3-30. All proton and carbon resonances of compound **5** were assigned by 2D-NMR experiments (^{1}H–^{1}H COSY, HSQC, HMBC) as reported in Table 1.

The proposed structure was supported by ^{1}H NMR and HRESIMS analyses of the acetyl derivative **5a**, which exhibited two acetyl groups confirming the presence of two secondary hydroxyl functions in aplysiol A (**5**).

Due to the close similarity of carbon and proton resonances of the fragment C-1/C-17 in **1** and **5**, the stereochemistry of this portion was assumed to be in **5** the same as **1**. The relative stereochemistry of the substituents in the five-membered ring was suggested by analysis of NMR spectroscopic values, as well as by NOE difference experiments. Significant differences were observed in the proton resonances of the tertiary methyls in the right-side end with respect to the corresponding values for thyrsiferol [H_3-24 and H_3-30 (δ 1.36 and δ 1.32 for **5**, δ 1.12 and δ 1.21 for **1**), H_3-29 (δ 1.38 for **5**, δ 1.15 for **1**)]. This could be explained by the deshielding effect of the hydroxyl group on the three methyls and should imply that the –OH at C-21 had the same orientation as both methyl and hydroxy-isopropyl groups at C-19 and C-22, respectively. Strong steric

Table 1. NMR data[a] of thyrsiferol[b] (**1**) and aplysiols A (**5**) and B (**6**)

Position	**1**			**5**			**6**		
	δ ^{1}H[d] m, Hz	δ ^{13}C[c]	HMBC[e]	δ ^{1}H[d] m, Hz	δ ^{13}C[c]	HMBC[e]	δ ^{1}H[d] m, Hz	δ ^{13}C[c]	HMBC[e]
1	1.40 s	23.6 q	$H_3$25, H3	1.40 s	23.7 q	$H_3$25, H3	1.40 s	24.1 q	$H_3$25, H3
2	—	74.9 s	$H_3$1, $H_3$25, H3	—	75.0 s	$H_3$1, $H_3$25, H3	—	74.9 s	$H_3$1, $H_3$25, H3
3	3.89 dd, 4.1, 12.3	59.0 d	$H_3$1, $H_3$25, $H_2$4	3.89 dd, 3.8,12.1	60.0 d	$H_3$1, $H_3$25, $H_2$4	3.89 dd, 4.1, 12.2	59.1 d	$H_3$1, $H_3$25, $H_2$4
4	2.24 m 2.07 m	28.2 t	H3, $H_2$5	2.22 m 2.10 m	28.2 t	H3, $H_2$5	2.22 m 2.10 m	28.2 t	H3, $H_2$5
5	1.79 m 1.52 m	37.0 t	$H_3$26	1.81 m 1.54 m	37.0 t	$H_3$26	1.82 m 1.53 m	37.1 t	$H_3$26
6	—	74.2 s	$H_3$26, H7	—	75.0 s	$H_3$26, H7	—	74.4 s	$H_3$26, H7
7	3.04 br d, 11.6	86.5 d	$H_3$26, $H_2$8	3.05 br d, 11.5	86.5 d	$H_3$26, $H_2$8	3.04 br d, 11.4	86.5 d	$H_3$26, $H_2$8
8	1.72 m	23.0 t	$H_2$9	1.73 m	23.0 t	$H_2$9	1.72 m	23.0 t	$H_2$9
9	1.78 m 1.53 m	38.5 t	$H_3$27	1.76 m 1.46 m	38.5 t	$H_3$27	1.71 m 1.41 m	38.6 t	$H_3$27
10	—	71.9 s	$H_3$27, H11	—	72.0 s	$H_3$27, H11	—	71.4 s	$H_3$27, H11
11	3.56 dd, 6.8, 10.6	76.3 d	$H_3$27, $H_2$12	3.56 m	76.3 d	$H_3$27, $H_2$12	3.55 dd, 7.0, 11.1	76.6 d	$H_3$27, $H_2$12
12	1.90 m 1.51 m	21.1 t	H11	1.90 m 1.50 m	21.1 t	H11	1.87 m 1.52 m	21.3 t	H11
13	1.57 m	25.5 t	$H_2$12	1.50 m	25.5 t	$H_2$12	1.80 m	21.4 t	$H_2$12
14	3.71 m	76.1 d	$H_3$28	3.71 dd, 2.5, 12.7	76.1 d	$H_3$28	3.71 m	75.4 d	$H_3$28
15	—	73.2 s	$H_3$28, $H_2$16	—	73.2 s	$H_3$28, $H_2$16	—	84.3 s	$H_3$28, $H_2$16
16	1.83 m 1.39 m	33.5 t	$H_3$28, $H_2$17	1.80 m 1.32 m	33.4 t	$H_3$28, $H_2$17	1.98 m 1.69 m	35.8 t	$H_3$28, $H_2$17
17	1.86 m 1.70 m	20.7 t	H18	1.78 m 1.67 m	20.7 t	H18	1.81 m —	25.9 t	H18
18	3.45 dd, 7.1, 14.3	77.6 d	$H_3$29, $H_2$17	3.45 dd, 1.6, 9.9	78.8 d	$H_3$29, $H_2$17	3.71 m	86.4 d	$H_3$29, H17
19	—	86.0 s	$H_3$29, H18, $H_2$20	—	86.0 s	$H_3$29, H18, $H_2$20	— m	72.3 s	$H_3$29, H18
20	2.10 m 1.62 m	32.3 t	$H_3$29, $H_2$21	2.20 m 1.81 m	41.5 t	$H_3$29, $H_2$21	1.57 m —	33.7 t	$H_3$29
21	1.85 m —	26.6 t	H22	4.45 br s —	74.3 d	H22	1.67 m 1.40 m	25.4 t	H22
22	3.76 br d, 6.5	87.4 d	$H_2$21, $H_3$24, $H_3$30	3.57 d, 1.5	87.0 d	$H_2$21, $H_3$24, $H_3$30	3.44 dd, 2.2, 10.4	78.4 d	$H_2$21, $H_3$24, $H_3$30
23	—	70.5 s	$H_3$24, $H_3$30	—	72.0 s	$H_3$24, $H_3$30	—	73.1 s	$H_3$24, $H_3$30
24	1.12[f] s	23.9[f] q	$H_3$30	1.36[f] s	24.2[f] q	$H_3$30	1.17[f] s	23.7[f] q	$H_3$30
25	1.27 s	31.0 q	$H_3$1, H3	1.27 s	31.0 q	$H_3$1, H3	1.27 s	31.0 q	$H_3$1, H3
26	1.20 s	20.1 q	H7	1.21 s	20.1 q	H7	1.20 s	20.1 q	H7
27	1.18 s	21.4 q	$H_2$9, H11	1.18 s	21.4 q	$H_2$9, H11	1.18 s	21.2 q	$H_2$9, H11
28	1.11 s	22.9 q	H14, $H_2$16	1.10 s	23.0 q	H14, $H_2$16	1.09 s	23.2 q	H14, H16
29	1.15 s	23.4 q	H18, $H_2$20	1.38 s	24.2 q	H18, $H_2$20	1.18 s	21.6 q	H18, $H_2$20
30	1.21[f] s	27.6[f] q	$H_3$24	1.32[f] s	29.2[f] q	$H_3$24	1.23[f] s	26.7[f] q	$H_3$24

[a] Bruker DRX-600 spectrometer, Bruker DPX-300 spectrometer in $CDCl_3$, chemical shifts (ppm) referred to $CHCl_3$ (δ 7.26) and to $CDCl_3$ (δ 77.0).
[b] Full assignments of protons and carbons have been done.
[c] By DEPT, HSQC and HMBC (J=10 Hz) experiments.
[d] By ^{1}H–^{1}H COSY and HSQC experiments.
[e] Significant HMBC correlations (J=10 Hz).
[f] Values in the same column are interchangeable.

Table 2. Selected ^{1}H NMR assignments[a] in $CDCl_3$ of **5b** ((*S*)-ester) and **5c** ((*R*)-ester)

	5b ((*S*)-ester)		**5c** ((*R*)-ester)		Δδ
	δ H	m (*J*, Hz)	δ H	m (*J*, Hz)	
H_2-16	1.80/1.53	m	1.80/1.60	m	0/−0.07
H_2-17	1.73	m	1.77	m	−0.04
H-18	5.01	dd (2.9, 9.1)	5.05	dd (3.3, 8.7)	−0.04
H_2-20	2.26/1.59	m	2.30/1.70	m	−0.04/−0.11
H-21	5.38	br s	5.40	br s	−0.02
H-22	3.62	br d (1.7)	3.60	br d (1.8)	+0.02
H_3-24	1.11	s	0.92	s	+0.19
H_3-28	1.00	s	1.04	s	−0.04
H_3-29	0.84	s	1.21	s	−0.37
H_3-30	1.14	s	1.01	s	+0.13

[a] Bruker DRX 600 spectrometer, in $CDCl_3$, chemical shifts (ppm) referred to $CHCl_3$ (δ 7.26) and to $CDCl_3$ (δ 77.0).

interactions were observed among H-21 (δ 4.45), H-22 (δ 3.57) and H_2-20a (δ 2.20), whereas clear NOE contacts between H-18 and H-22 were not detected, due to the similar ^{1}H NMR chemical shifts of these two protons. In order to get further information on the stereochemistry, we decided to apply the Mosher's method. Compound **5** was treated with (*R*)- and (*S*)-MTPA chlorides in dry methylene chloride and DMAP to give the corresponding (*S*)-MTPA (**5b**) and (*R*)-MTPA (**5c**) esters that were fully characterised by 2D-NMR (selected ^{1}H NMR values are listed in Table 2).

Some NOE difference experiments were also conducted on the (*R*)-ester (**5c**) confirming the suggested orientation for the substituents in the five-membered ring. In fact, a diagnostic effect was observed between H-18 (δ 5.05) and H-22 (δ 3.60), and between H_2-20a and H-18, H-21 and H-22, according to the proposed relative stereochemistry. The Δδ values generated in (*S*)- and (*R*)-ester for the signals of protons nearby the hydroxyl groups at C-18 and C-21 are reported in Figure 1.

Taking into account that in polyderivatised compounds the Δδ values observed are the results of the combined effects (shielding/dieshielding) of all the MTPA phenyl rings,[13] the good homogeneity of the $\Delta\delta^{SR}$ signs observed around C-21 allowed to assign to this centre the *S* configuration. In fact, if the absolute stereochemistry at C-18 is *S*, the negative $\Delta\delta^{SR}$ observed for carbons 19, 20 and 21 can be justified only by assigning the same stereochemistry at C-22. Analogously, with the *R* stereochemistry at C-18, the positive $\Delta\delta^{SR}$ observed at carbons 22, 23, 24 and 30 are justified only by assigning the *S* configuration at C-22. An apparent anomaly was observed for C-18, for which the negative $\Delta\delta^{SR}$ of H_3-29 and H_2-20 were due most likely to the opposite influence of MTPA derivatization at the other hydroxyl group at C-21. However, the negative $\Delta\delta^{SR}$ at C-28, C-15, C-16 and C-17 led us to propose an *S* stereochemistry also for C-18, in agreement with the configuration of thyrsiferol (**1**). The absolute stereochemistry at all the remaining chiral centres of the molecule was assumed to be the same as **1** by biogenetical considerations.

The molecular formula of aplysiol B (**6**), $C_{30}H_{53}BrO_7$, deduced by HRESIMS on the sodiated molecular ion at 627.2879, indicated that it was an isomer of thyrsiferol (**1**). Analysis of ^{1}H and ^{13}C NMR spectra of **6** revealed a different arrangement of C-15/C-24 portion in the molecule, with respect to thyrsiferol (**1**). In addition to the signals due to the bromine-containing pyran and dioxabicyclo[4,4,0]decane rings on the left side of the molecule, NMR spectra of **6** showed signals attributable to four CH_2 and four tertiary CH_3, along with two methines and three quaternary carbons all linked to oxygen. Analogously with thyrsiferol (**1**), an additional ring was present in this part of the molecule as required by the molecular formula. Two isolated spin systems were easily recognised by analysis of ^{1}H–^{1}H COSY and HSQC spectra. In particular, one of them was formed by a diastereotopic methylene resonating at δ 1.98 and δ 1.69 (H_2-16) coupled to a methylene at δ 1.81 (H_2-17), which was further correlated to a methine at δ 3.71 (H-18), whereas the other system was constituted by a methylene centred at δ 1.57 (H_2-20) displaying cross-peaks with a diastereotopic methylene at δ 1.67 and δ 1.40 (H_2-21), which was in turn coupled to a methine at δ 3.44 (H-22). The HMBC data allowed the connection of these two partial structures to the quaternary carbons and to the methyl groups. In particular, diagnostic HMBC correlations were observed between C-15 and H-14, H_2-16 and H_3-28, between C-19 and H-18, H_2-20 and H_3-29, and between C-23 and H-22, H_3-24 and H_3-30, leading to the sequence **a** as indicated in Figure 2. Thyrsiferol displays the same sequence, because of this the structural differences between **1** and **6** should be due to different cyclisations. The comparison of the NMR values with those reported for model compounds as well as the analysis of the ^{1}H NMR spectrum of the acetyl derivative of **6**, compound **6a**, strongly suggested the presence of a tetrahydrofuran ring in this moiety, with the

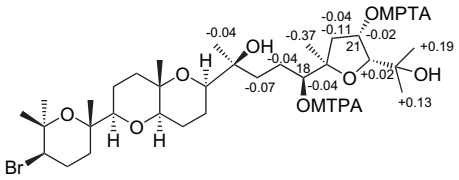

Figure 1. $\Delta\delta^{SR}$ for the Mosher derivatives of **5**.

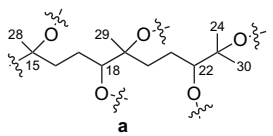

Figure 2. Substructure **a** (C-15/C-24) in aplysiol B (**6**).

oxygen bridge between C-15 (δ_C 84.3) and C-18 (δ_C 86.4) and a unique secondary hydroxyl group at C-22. In fact, in the ^{1}H NMR spectrum of the acetyl derivative **6a**, only one acetyl signal was present at δ 2.10, whereas H-22 resonated at δ 4.81 by the acylation shift effect.

All proton and carbon values were assigned by 2D-NMR experiments and were in agreement with the proposed structure **6**. With the aim at establishing the stereochemistry at the 10 stereogenic centres (C-3, C-6, C-7, C-10, C-11, C-14, C-15, C-18, C-19 and C-22) of aplysiol B (**6**), a configurational study by an integrated NMR-QM (Quantum Mechanical) approach,[14,15] based on the combination of ^{13}C NMR chemical shifts and $^{2,3}J_{C-H}$ coupling constant DFT (density functional theory) calculations and the analysis of the experimental NMR data, was undertaken.

In particular, both ^{13}C and $^{2,3}J_{C-H}$ experimental values were used to validate the theoretical models, and dipolar coupling correlations derived from 2D-ROESY NMR experiments were used to corroborate the arrangement suggested by QM methods, and to determine the relative configuration of the rigid portions of the molecule. Finally, the Mosher's method was employed to confirm the absolute configuration of C-22.

Compound **6** is biogenetically correlated to **1**, the absolute configuration of which has been determined by stereospecific synthesis.[16] As reported above, the NMR investigation revealed that aplysiol B (**6**) and thyrsiferol (**1**) have an identical, rigid left-side moiety (Table 1, C-1/C-14). For structure **6**, the relative configuration of the left-side moiety was confirmed by ROESY experiments. In detail, H-3 presented strong dipolar couplings with H_3-25, H-4β and H-5β, whereas H_3-1 gave rise to ROE correlations with H-5α and H_3-26. There was also a dipolar coupling between H_3-26 and H-5α, which confirmed the relative configuration of the brominated ring. Finally, ROE correlations of H-7 with H-8β and H-11, and the dipolar couplings of H-11 with H-12β and H-14 were indicative of the relative configuration of bicyclic portion. On the basis of biogenetic consideration, in our calculations we considered for this identical left-side moiety the same absolute configuration as **1**.

Following a recent strategy based on the QM calculation of *J* couplings for the determination of the relative configuration of adjacent couple of stereocentres,[17] we examined the arrangement of the C_2 fragments C-14/C-15 and C-18/C-19.

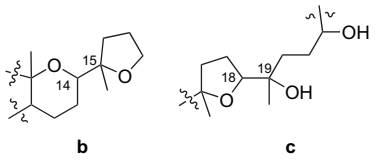

b **c**

Figure 3. Molecular fragments **b** and **c** representing the reduced systems of **6** including the portions C-14/C-15 and C-18/C-19, respectively.

In accordance with the above mentioned procedure, we considered two molecular fragments,[17] which represent a simplification of the entire molecule (Fig. 3); of such fragments we took into account the two possible diastereomers *erythro* and *threo*, and all the three staggered rotamers (g+, g− and *anti*) for each diastereomer. While in the original paper it is proposed to substitute to the main chain at least two heavy groups (carbon, oxygen atoms), and to every branched chain at least one heavy atom, in our case for both fragments C-14/C-15 and C-18/C-19 some of the stereogenic carbons were part of a cycle; for this reason we included in our calculation the complete ring portions including the stereogenic atoms, going well over the lowest requirements suggested in the previous paper.[17]

Each of the six conformers, three for the *erythro* and three for the *threo* arrangement, was optimised at MPW1PW91 level of theory using the 6-31G(d) basis set; the calculation of *J* couplings was executed on the so-obtained geometries using the same functional and the 6-31G(d,p) basis set. In Table 3 are reported the experimental and calculated *J*-coupling constants for the various conformational and configurational arrangements.

In Table 3 are reported the results of the above described *J* calculations for the six possible arrangements in comparison with the experimental data. For the fragment C-14/C-15, two of the six arrangements, the calculated *J* values, namely the *anti threo* and the *anti erythro*, are in good agreement with the experimental ones, by showing the lowest sum of absolute errors $\Sigma|J\text{calcd}-J\text{exp}|$ (Total Absolute Deviation values, TAD) in the reproduction of experimental *J* data; it is noteworthy that for such arrangements, all the single calculated *J* values differ from the experimental for less than 1 Hz. Differently from the original *J*-based approach proposed by Murata et al.,[18] for which it is impossible to distinguish the *anti erythro* from the *anti threo* arrangement on the basis of the sole evaluation of the *J*-coupling values, in this

Table 3. Calculated (MPW1PW91/6-31G(d,p) level) $^{2,3}J_{C-H}$ coupling constants of aplysiol B (**6**) for the six conformational arrangements belonging to *erythro* and *threo* series in comparison with the experimental data: single deviations and TAD ($\Sigma|J_{calcd}-J_{exp}|$) values

	g+	*erythro*	Calcd		*threo*	g−	Exp
		anti	g−	g+	*anti*		
b (C14–15)							
$^2J_{C15-H14}$	−3.1	1.5	−1.8	−3.1	2.3	−2.1	2.3
$^3J_{C16-H14}$	2.7	1.1	2.6	1.2	0.6	3.0	0.9
$^3J_{Me-H14}$	1.8	0.7	2.9	2.9	1.3	3.1	0.3
TAD	8.7	**1.4**	8.3	8.2	**1.3**	9.2	
c (C18–C19)							
$^2J_{C19-H18}$	−0.8	0.3	5.2	−0.1	5.5	−0.2	0.8
$^3J_{C20-H18}$	2.5	3.4	0.8	1.5	1.2	3.8	0.6
$^3J_{Me-H18}$	2.1	2.9	1.4	2.5	0.9	4.6	2.5
TAD	3.9	5.7	3.8	**1.9**	6.8	6.4	

case the quantitative analysis of the calculated versus the experimental data allows to observe a slightly better agreement for the *anti threo* arrangement. To confirm such observation, a complementary analysis of the ROESY data was carried on, revealing crucial dipolar correlations between H-14 and H_3-23 and H-16α, and between H_3-23 and H-13, so confirming the *anti threo* arrangement supported by the *J*-based results. On the basis of the knowledge of the absolute configuration of C-14, the *RR* configuration of the fragment C-14/C-15 was assigned.

The analysis of the C_2 fragment C-18/C-19 (see Table 3) revealed that only the g+ rotamer of *threo* arrangement was in good agreement with experimental *J* values. Moreover, the g+ rotamer of *threo* arrangement presented single differences between calculated and experimental *J* values lower than 1 Hz, whereas for all the other rotamers significant differences were found in comparison with the experimental data. Finally, the evaluation of the ROESY data revealed the presence of dipolar couplings between H-18 and H_3-29 and H_2-20, and between H-17 and H_2-20 confirming the *J*-based results and allowing to assign the *threo* configuration for the fragment C-18/C-19.

In order to determine the configuration of the tetrahydrofuran ring, and so the relationship between C-15 and C-18, a careful examination of the 2D-ROESY data was carried out. In particular, the strong dipolar couplings between H-14 and H_3-28 and H-16α (Fig. 4), between H-16β and H_3-28, and between H-18 and H-16α allowed to establish the *R* absolute configuration of C-18, and, following the information derived from the above *J*-based analysis, the consequent *R* configuration for C-19.

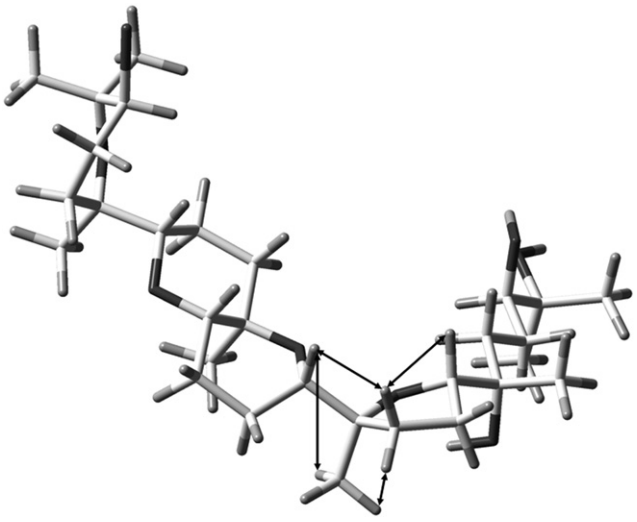

Figure 4. Significant experimental ROEs (black arrows) for the configuration assignment of C-15 and C-18.

Once the 14(*R*), 15(*R*), 18(*R*), 19(*R*) configuration was assessed, and in order to obtain information about the configuration of C-22, we built the two possible models **6** and **7** (Fig. 5), having the 14(*R*), 15(*R*), 18(*R*), 19(*R*), 22(*S*) and the 14(*R*), 15(*R*), 18(*R*), 19(*R*), 22(*R*) configuration, respectively. For such models, we calculated the ^{13}C NMR chemical shifts at quantum mechanical level and subsequently compared the results with the experimental data, following a protocol proposed by one of the authors (G.B.),[14] which has been applied for assigning the relative configuration of several natural compounds.[15]

In detail, a conformational search of the two models by molecular mechanics (MonteCarlo Multiple Minimum method of the MacroModel package, see Section 3)[22] was performed. All the significant conformers of the two diastereoisomers were subsequently optimised at DFT level using the MPW1PW91 functional and the 6-31G(d) basis set. On the so-obtained geometries, single point calculation of the ^{13}C chemical shifts were performed, using the same functional and the 6-31G (d,p) basis set; the final chemical shift values for each diastereoisomers were derived taking into account the Boltzmann weighted average based on the energies of the single conformers for each stereoisomer.

The resulting ^{13}C NMR chemical shifts corresponding to the models **6** and **7** were compared with the experimental ones; in Table 4 are reported the calculated versus the experimental values, together with the mean absolute errors for each stereoisomer.

Table 4. Significant ^{13}C NMR calculated (MPW1PW91/6-31G(d,p) level) chemical shifts for **6** and **7**, and the corresponding ^{13}C NMR (δ, ppm) experimental data of aplysiol B

Atom	Calculated ^{13}C chemical shifts		Exp.
	6	**7**	
12	26.6	26.7	21.3
13	25.7	26.2	21.4
14	78.1	76.5	75.4
15	82.7	82.9	84.3
18	86.4	87.7	86.4
17	28.3	27.9	25.9
16	35.1	33.9	35.8
28	28.5	26.4	23.2
19	73.2	70.0	72.3
29	19.8	22.2	21.6
20	34.4	40.1	33.7
21	27.4	28.4	25.4
22	72.5	74.6	78.4
23	70.9	70.6	73.1
MAE[a]	**2.56**	2.84	

[a] Mean absolute error (MAE) found for ^{13}C NMR chemical shifts of compounds **6** and **7** versus ^{13}C experimental values: $MAE=\sum[|(\delta_{exp}-\delta_{calcd})|]/n$.

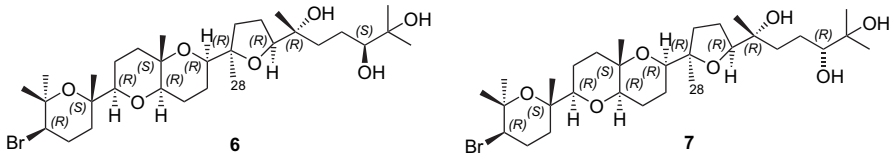

Figure 5. Two stereoisomer models, **6** and **7**, considered for quantum mechanical calculations of ^{13}C NMR chemical shifts.

As shown in Table 4, **6** shows an MAE value of 2.56 versus 2.84 for **7**, suggesting the *S* configuration for C-22. It is noteworthy that the MAE value of 2.56 is in good agreement with the MAE value of 2.48, obtained at the same level of theory for a set of known natural compounds;[19] for this reason such result not only provides information on the *S* configuration of C-22, but also corroborates the configurational arrangement of C-14, C-15, C-18 and C-19 depicted in **6** and determined as described above.

A final contribution to this stereochemical analysis was provided by the application of the Mosher's method. Treatment of compound **6** with (*R*)- and (*S*)-MTPA chlorides in dry methylene chloride and DMAP afforded the corresponding (*S*)-MTPA (**6b**) and (*R*)-MTPA (**6c**) esters, respectively. The two Mosher derivatives were fully characterised by 2D-NMR experiments (^{1}H–^{1}H COSY, HSQC, HMBC), some selected ^{1}H NMR data and $\Delta\delta$ ($\delta S-\delta R$) are reported in Table 5.

The $\Delta\delta$ values observed for the signals of protons nearby the hydroxyl group at C-22 indicated the *S* configuration for this centre, as depicted in formula **6**, finally confirming the absolute stereochemistry proposed.

The selective presence of compounds **5** and **6** on the mantle of the sea hare *A. dactylomela* suggested an involvement of these molecules in the chemical defensive mechanisms of the mollusc. Thus, feeding-deterrence and ichthyotoxicity properties of both compounds were evaluated according to the literature procedures.[20,21] Compounds **5** and **6** were active at 50 μg/cm^2 in the feeding-deterrence test against gold fish *Carassius auratus*,[20] and toxic at a concentration of 10 ppm in the ichthyotoxicity assay on *Gambusia affinis*,[21] strongly supporting their possible defensive role.

In conclusion, in this paper we have described the structure and the absolute stereochemistry of two triterpenes, aplysiols A (**5**) and B (**6**) that have been elucidated by NMR techniques as well as by an integrated NMR-QM (Quantum Mechanical) method. Compounds **5** and **6**, which were selectively located on the mantle of *A. dactylomela*, are structurally related to thyrsiferol (**1**), a known algal metabolite. In particular, compound **5** is the C-21 hydroxyl derivative of **1** whereas compound **6** exhibits a different arrangement in the right side of the molecule. A plausible biogenetic pathway (Fig. 6), leading to compound **6**, should involve a nucleophilic attachment of two molecules of water followed by a series of ring closings favoured by bromine ion electrophilic attachment on a squalene tetraepoxide, analogously with thyrsiferol.[1]

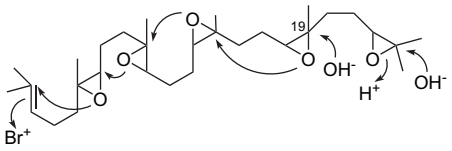

Figure 6. Possible biogenetic pathway to get compound **6**.

3. Experimental section

3.1. General experimental procedures

TLC plates (Merck Silica Gel 60 F_{254}) were used for analytical TLC and Merck Kieselgel 60 was used for preparative column chromatography. HRESIMS were carried out on a Micromass Q-TOF micro. HPLC Waters 501 pumps with a refractometer detector was used, equipped with direct-phase column Kromasil Silica, 5μ (250×4.60 mm, Phenomenex). NMR spectra, recorded at the NMR Service of Istituto di Chimica Biomolecolare of CNR (Pozzuoli, Italy), were acquired on a Bruker Avance-DRX600 operating at 600 MHz, in $CDCl_3$ (δ values are reported referred to C*H*Cl$_3$ at 7.26 ppm), using an inverse TCI Cryo Probe fitted with a gradient along the *z*-axis. ^{13}C NMR spectra were recorded on a Bruker DPX-300 operating at 300 MHz (δ values are reported to C*D*Cl$_3$, 77.0 ppm) using a dual probe. NMR spectra, recorded at the Dipartimento di Scienze Farmaceutiche, Universita' di Salerno (Salerno, Italy), were also acquired on a Bruker Avance-DRX600 operating at 600 MHz, in $CDCl_3$ (δ values are reported referred to C*H*Cl$_3$ at 7.26 ppm), using an inverse TCI Cryo Probe fitted with a gradient along the *z*-axis. Optical rotations were measured on a Jasco DIP 370 digital polarimeter. IR spectra were measured on a Biorad FTS 155 FTIR spectrophotometer.

3.2. Extraction and isolation procedure

The collection and extraction of *A. dactylomela* (four individuals) have been already described.[11]

The ether extracts of the two dissected anatomical parts (mantle and internal organs) were subjected to silica gel column chromatography, giving, along with halogenated acetogenins previously reported,[11] similar terpenoid fractions at R_f 0.20–0.40 (eluent: $CHCl_3$/MeOH 95:5), furthermore purified by reverse phase HPLC (MeOH/H_2O, 85/15).

Thyrsiferol (**1**): oil, R_f 0.33 ($CHCl_3$/MeOH 95:5); $[\alpha]_D$ +28 (*c* 0.6, $CHCl_3$); HRESIMS *m/z* 627.2870 (M+Na), calcd

Table 5. Selected ^{1}H NMR selective assignments[a] in $CDCl_3$ of **6b** ((*S*)-ester) and **6c** ((*R*)-ester)

	6b ((*S*)-ester)		**6c** ((*R*)-ester)		$\Delta\delta$
	δ H	m (*J*, Hz)	δ H	m (*J*, Hz)	
H_2-20	1.12	m	1.24	m	−0.12
H_2-21	1.83/1.57	m	1.95/1.64	m	−0.12/−0.07
H-22	4.99	br d (9.1)	5.01	br d (10.4)	−0.02
H_3-24	1.17	s	1.16	s	+0.01
H_3-29	1.02	s	1.08	s	−0.06
H_3-30	1.24	s	1.20	s	+0.04

[a] Bruker DRX 600 spectrometer, in $CDCl_3$, chemical shifts (ppm) referred to $CHCl_3$ (δ 7.26) and to $CDCl_3$ (δ 77.0).

for $C_{30}H_{53}{}^{79}BrO_7$+Na 627.2874. ^1H and ^{13}C NMR data in Table 1.

Venustatriol (**2**): oil, R_f 0.35 ($CHCl_3$/MeOH 95:5); $[\alpha]_D$ +8.0 (*c* 0.1, $CHCl_3$); HRESIMS *m/z* 627.2869 (M+Na), calcd for $C_{30}H_{53}{}^{79}BrO_7$+Na 627.2874. ^1H and ^{13}C NMR data were identical to those of the literature.[4]

Aplysiol A (**5**): oil, R_f 0.25 ($CHCl_3$/MeOH 95:5); $[\alpha]_D$ +2.0 (*c* 0.7, $CHCl_3$); HRESIMS *m/z* 643.2828 (M+Na), calcd for $C_{30}H_{53}{}^{79}BrO_8$+Na 643.2824. ^1H and ^{13}C NMR data in Table 1.

Aplysiol B (**6**): oil, R_f 0.3 ($CHCl_3$/MeOH 95:5); $[\alpha]_D$ −9.0 (*c* 0.9, $CHCl_3$); HRESIMS *m/z* 627.2879 (M+Na), calcd for $C_{30}H_{53}{}^{79}BrO_7$Na 627.2874. ^1H and ^{13}C NMR data in Table 1.

Acetylated aplysiol A (**5a**): aplysiol A (**5**) (0.3 mg) was treated with acetic anhydride (0.2 ml) in dry pyridine (0.5 ml) for about 14 h under stirring at room temperature. The compound was purified by chromatography in a Pasteur pipette (SiO_2, chloroform). HRESIMS *m/z* 727.3137 (M+Na), calcd for $C_{34}H_{57}{}^{79}BrO_{10}$Na 727.3142. Selected ^1H NMR ($CDCl_3$) data: δ 5.36 (1H, br s, H-21), δ 4.91 (1H, m, H-18), δ 3.89 (1H, dd, J=5.2 and 12.2 Hz, H-3), δ 3.71 (1H, m, H-14), δ 3.65 (1H, d, J=1.8 Hz H-22), δ 3.56 (1H, m, H-11), δ 3.05 (1H, br d, J=11.4 Hz, H-7), δ 2.08 (3H, s, H_3-OAc), δ 2.06 (3H, s, H_3-OAc).

Acetylated aplysiol B (**6a**): aplysiol B (**6**) (0.3 mg) was treated with acetic anhydride (0.2 ml) in dry pyridine (0.5 ml) for about 14 h under stirring at room temperature. The compound was purified by chromatography in a Pasteur pipette (SiO_2, chloroform). HRESIMS *m/z* 669.2991 (M+Na), calcd for $C_{32}H_{55}{}^{79}BrO_8$Na 669.2987. Selected ^1H NMR ($CDCl_3$) data: δ 4.81 (1H, dd, J=2.5 and 10.2 Hz, H-22), δ 3.89 (1H, dd, J=2.5 and 10.1 Hz, H-3), δ 3.71 (2H, m, H-14, H-18), δ 3.55 (1H, m, H-11), δ 3.04 (1H, br d, J=10.8 Hz, H-7), δ 2.10 (3H, s, H_3-OAc), δ 1.40 (3H, s, H_3-25), δ 1.27 (3H, s, H_3-1), δ 1.23 (3H, s, H_3-24), δ 1.20 (3H, s, H_3-26), δ 1.18 (3H, s, H_3-27), δ 1.17 (6H, s, H_3-29, H_3-30), δ 1.09 (3H, s, H_3-28).

3.3. Preparation of MTPA esters

Compound **5b** ((*S*)-MTPA ester): the compound was prepared by treating aplysiol A (**5**) (2 mg) with (*R*)-(−)-MTPA chloride (0.05 ml) in dry methylene chloride (1 ml) with catalytic amount of DMAP for about 16 h under stirring at room temperature. The ester was purified by chromatography in a Pasteur pipette (SiO_2, chloroform). Selected ^1H NMR values are in Table 2.

Compound **5c** ((*R*)-MTPA ester): the compound was prepared by treating the aplysiol A (**5**) (2 mg) with (*S*)-(−)-MTPA chloride (0.05 ml) in dry methylene chloride (1 ml) with catalytic amount of DMAP for about 16 h under stirring at room temperature. The ester was purified by chromatography in a Pasteur pipette (SiO_2, chloroform). Selected ^1H NMR values are in Table 2.

Compound **6b** ((*S*)-MTPA ester): the compound was prepared by treating aplysiol B (**6**) (2 mg) with (*R*)-(−)-MTPA chloride (0.05 ml) in dry methylene chloride (1 ml) with catalytic amount of DMAP for about 16 h under stirring at room temperature. The ester was purified by chromatography in a Pasteur pipette (SiO_2, chloroform). Selected ^1H NMR values are in Table 5.

Compound **6c** ((*R*)-MTPA ester): the compound was prepared by treating the aplysiol A (**5**) (2 mg) with (*S*)-(−)-MTPA chloride (0.05 ml) in dry methylene chloride (1 ml) with catalytic amount of DMAP for about 16 h under stirring at room temperature. The ester was purified by chromatography in a Pasteur pipette (SiO_2; chloroform). Selected ^1H NMR values are in Table 5.

3.4. Computational details

Molecular mechanics (MM) calculations were performed on a Pentium IV 2800 MHz using the MacroModel 8.5 software[22] package and the MMFFs force field.[23] MonteCarlo Multiple Minimum (MCMM) method (10,000 steps) of the MacroModel package[22] was used in order to allow a full exploration of the conformational space. All the structures so-obtained were optimised using the Polak–Ribier Conjugate Gradient algorithm (PRCG, 1000 steps, maximum derivative less than 0.05 kcal/mol). This led to the selection of the lowest energy minimum conformer for **6**. The initial geometries of the minimum energy conformers for **6** were optimised at the hybrid DFT MPW1PW91 level using the 6-31G(d) basis set (Gaussian 03 Software Package).[24] GIAO ^{13}C and *J*-coupling calculations were performed using the MPW1PW91 functional and the 6-31G(d,p) basis set, using as input the geometry previously optimised at MPW1PW91/6-31G(d) level.

3.5. NMR experiments

NMR experiments were recorded on a Bruker DRX600 spectrometer at T=300 K. All spectra were acquired in the phase-sensitive mode and the TPPI method was used for quadrature detection in the ω_1 dimension. The compound was dissolved in 0.5 ml of $CDCl_3$ 99.96%. The spectra were calibrated using the solvent signal as internal standard (^1H, δ=7.26 ppm; ^{13}C, δ=77.0 ppm).

The ROESY[25] spectrum was executed with a number of 128 scans/t_1, a t_{1max} value of 111.08 ms and a mixing time of 400 ms.

The ω_1-half-filtered TOCSY (HETLOC)[26] spectrum was executed with a number of 96 scans/t_1, a t_{1max} value of 71.09 ms.

Phase-sensitive (PS)–Pulse Field Gradient (PFG)–HMBC[27] spectrum was executed with a number of 256 scans/t_1, a t_{1max} value of 2.37 ms.

The NMR data were processed on a Silicon Graphic Indigo2 workstation using UXNMR software.

Acknowledgements

We thank D. Ricciardi for technical assistance and R. Turco for drawing. The NMR spectra were recorded at the ICB

NMR Service, the staff of which is acknowledged. Particular thanks are due to D. Melck of the staff service. This research has been partially funded by an Italian–Chinese bilateral project and by Chinese Marine 863 projects 2006AA-09Z412 and 2006AA09Z447.

References and notes

1. Fernández, J. J.; Souto, M. L.; Norte, M. *Nat. Prod. Rep.* **2000**, *17*, 235–246.
2. Blunt, J. W.; Copp, B. R.; Munro, M. H. G.; Nothcote, P. T.; Prinsep, M. R. *Nat. Prod. Rep.* **2006**, *23*, 26–78 and previous articles in the same series.
3. Blunt, J. W.; Hartshorn, M. P.; McLennan, T. J.; Munro, M. H. G.; Robinson, W. T.; Yorke, S. C. *Tetrahedron Lett.* **1978**, 69–72.
4. Sakemi, S.; Higa, T.; Jefford, C. W.; Bernardinelli, G. *Tetrahedron Lett.* **1986**, *27*, 4287–4290.
5. Manríquez, C. P.; Souto, M. L.; Gavín, J. A.; Norte, M.; Fernández, J. J. *Tetrahedron* **2001**, *57*, 3117–3123.
6. Norte, M.; Fernández, J. J.; Souto, M. L. *Tetrahedron Lett.* **1996**, *37*, 2671–2674.
7. Suzuki, T.; Suzuki, M.; Furusaki, A.; Matsumoto, T.; Kato, A.; Imanaka, Y.; Kurosawa, E. *Tetrahedron Lett.* **1985**, *26*, 1329–1332; Fernandez, J. J.; Souto, M. L.; Norte, M. *Bioorg. Med. Chem.* **1998**, 2237–2243.
8. Matsuzawa, S.; Suzuki, T.; Suzuki, M.; Matsuda, A.; Kawamura, T.; Mizuno, Y.; Kikuchi, K. *FEBS Lett.* **1994**, *356*, 272–274.
9. Broka, C. A.; Hu, L.; Lee, W. J.; Shen, T. *Tetrahedron Lett.* **1987**, *42*, 4993–4996; Corey, E. J.; Ha, D. C. *Tetrahedron Lett.* **1988**, *26*, 3171–3174; Hashimoto, M.; Kann, T.; Nozaki, K.; Yanagiya, M.; Shirahama, H.; Matsumoto, T. *Tetrahedron Lett.* **1988**, *29*, 1143–1144; Hashimoto, M.; Kann, T.; Nozaki, K.; Yanagiya, M.; Shirahama, H.; Matsumoto, T. *J. Org. Chem.* **1990**, *55*, 5088–5107; Gonzalez, I. C.; Forsyth, C. J. *Org. Lett.* **1999**, *1*, 319–322; Gonzalez, I. C.; Forsyth, C. J. *J. Am. Chem. Soc.* **2000**, *122*, 9099–9108.
10. Cimino, G.; Ciavatta, M. L.; Fontana, A.; Gavagnin, M. *Bioactive Compounds from Natural Sources*; Tringali, C., Ed.; Taylor and Francis: London and New York, NY, 2001; Vol. 15, pp 577–637.
11. Manzo, E.; Ciavatta, M. L.; Gavagnin, M.; Puliti, R.; Mollo, E.; Guo, Y. W.; Mattia, C. A.; Mazzarella, L.; Cimino, G. *Tetrahedron* **2005**, *61*, 7456–7460.
12. Blunt, J. W.; McCombs, J. D.; Munro, M. H. G.; Thomas, F. N. *Magn. Reson. Chem.* **1989**, *27*, 792–795.
13. Seco, J. M.; Quinoa, E.; Riguera, R. *Chem.Rev.* **2004**, *104*, 17–117.
14. Barone, G.; Duca, D.; Silvestri, A.; Gomez-Paloma, L.; Riccio, R.; Bifulco, G. *Chem.—Eur. J.* **2002**, *8*, 3240–3245.
15. Plaza, A.; Piacente, S.; Perrone, A.; Hamed, A.; Pizza, C.; Bifulco, G. *Tetrahedron* **2004**, *60*, 12201–12209; Riccio, R.; Bifulco, G.; Cimino, P.; Bassarello, C.; Gomez-Paloma, L. *Pure Appl. Chem.* **2003**, *75*, 295–308; Bassarello, C.; Bifulco, G.; Montoro, P.; Skhirtladze, A.; Kemertelidze, E.; Pizza, C.; Piacente, S. *Tetrahedron* **2006**, *63*, 148–154.
16. (a) Hashimoto, M.; Kan, T.; Nozaki, K.; Yanagiya, M.; Shirahama, H.; Matsumoto, T. *Tetrahedron Lett.* **1988**, *29*, 1143–1144; (b) Hashimoto, M.; Kan, T.; Nozaki, K.; Yanagiya, M.; Shirahama, H.; Matsumoto, T. *J. Org. Chem.* **1990**, *55*, 5088–5107.
17. Bifulco, G.; Bassarello, C.; Riccio, R.; Gomez-Paloma, L. *Org. Lett.* **2004**, *6*, 1025–1028.
18. Matsumori, N.; Kaneno, D.; Murata, M.; Nakamura, H.; Tachibana, K. *J. Org. Chem.* **1999**, *64*, 866–876.
19. Cimino, P.; Gomez-Paloma, L.; Duca, D.; Riccio, R.; Bifulco, G. *Magn. Reson. Chem.* **2004**, *42*, 26–33.
20. Cimino, G.; De Rosa, S.; De Stefano, S.; Sodano, G. *Comp. Biochem. Physiol., B* **1982**, *73*, 471–474.
21. Gunthorpe, L.; Cameron, A. M. *Mar. Biol.* **1987**, *94*, 39–43.
22. *MacroModel, version 8.5*; Schrödinger LLC: New York, NY, 2003.
23. Mohamadi, F.; Richards, N. G.; Guida, W. C.; Liskamp, R.; Lipton, M.; Caufield, C.; Chang, G.; Hendrickson, T.; Still, W. C. *J. Comput.Chem.* **1990**, *11*, 440–467.
24. Frisch, M. J.; Trucks, G. W.; Schlegel, H. B.; Scuseria, G. E.; Robb, M. A.; Cheeseman, J. R.; Montgomery, J. A., Jr.; Vreven, T.; Kudin, K. N.; Burant, J. C.; Millam, J. M.; Iyengar, S. S.; Tomasi, J.; Barone, V.; Mennucci, B.; Cossi, M.; Scalmani, G.; Rega, N.; Petersson, G. A.; Nakatsuji, H.; Hada, M.; Ehara, M.; Toyota, K.; Fukuda, R.; Hasegawa, J.; Ishida, M.; Nakajima, T.; Honda, Y.; Kitao, O.; Nakai, H.; Klene, M.; Li, X.; Knox, J. E.; Hratchian, H. P.; Cross, J. B.; Adamo, C.; Jaramillo, J.; Gomperts, R.; Stratmann, R. E.; Yazyev, O.; Austin, A. J.; Cammi, R.; Pomelli, C.; Ochterski, J. W.; Ayala, P. Y.; Morokuma, K.; Voth, G. A.; Salvador, P.; Dannenberg, J. J.; Zakrzewski, V. G.; Dapprich, S.; Daniels, A. D.; Strain, M. C.; Farkas, O.; Malick, D. K.; Rabuck, A. D.; Raghavachari, K.; Foresman, J. B.; Ortiz, J. V.; Cui, Q.; Baboul, A. G.; Clifford, S.; Cioslowski, J.; Stefanov, B. B.; Liu, G.; Liashenko, A.; Piskorz, P.; Komaromi, I.; Martin, R. L.; Fox, D. J.; Keith, T.; Al-Laham, M. A.; Peng, C. Y.; Nanayakkara, A.; Challacombe, M.; Gill, P. M. W.; Johnson, B.; Chen, W.; Wong, M. W.; Gonzalez, C.; Pople, J. A. *Gaussian 03, revision B.05*; Gaussian: Pittsburgh, PA, 2003.
25. Bax, A.; Davis, D. G. *J. Magn. Reson.* **1985**, *63*, 207–213.
26. Kurz, M.; Schmieder, P.; Kessler, H. *Angew. Chem., Int. Ed. Engl.* **1991**, *30*, 1329–1331.
27. Boyd, J.; Soffe, N.; John, B.; Plant, D.; Hurd, R. *J. Magn. Reson.* **1992**, *98*, 660–664; Davis, A. L.; Keeler, J.; Laue, E. D.; Moskau, D. *J. Magn. Reson.* **1992**, *98*, 207–216; Rinaldi, P. L.; Keifer, P. *J. Magn. Res., Ser. A* **1994**, *108*, 259–262.